

45 Years of Rotation of the Crab pulsar

A. G. Lyne^{1,*}, C. A. Jordan¹, F. Graham-Smith¹,
 C. M. Espinoza^{1,2}, B. W. Stappers¹ and P. Weltevrede¹

¹ *Jodrell Bank Centre for Astrophysics, School of Physics and Astronomy, The University of Manchester, Manchester M13 9PL, UK*

² *Instituto de Astrofísica, Facultad de Física, Pontificia Universidad Católica de Chile, Casilla 306, Santiago 22, Chile*

ABSTRACT

The 30-Hz rotation rate of the Crab pulsar has been monitored at Jodrell Bank Observatory since 1984 and by other observatories before then. Since 1968, the rotation rate has decreased by about 0.5 Hz, interrupted only by sporadic and small spin up events (glitches). 24 of these events have been observed, including a significant concentration of 15 occurring over an interval of 11 years following MJD 50000. The monotonic decrease of the slowdown rate is partially reversed at glitches. This reversal comprises a step and an asymptotic exponential with a 320-day time constant, as determined in the three best-isolated glitches. The cumulative effect of all glitches is to reduce the decrease in slowdown rate by about 6%. Overall, a low mean braking index of 2.342(1) is measured for the whole period, compared with values close to 2.5 in intervals between glitches. Removing the effects of individual glitches reveals an underlying power law slowdown with the same braking index of 2.5. We interpret this value in terms of a braking torque due to a dipolar magnetic field in which the inclination angle between the dipole and rotation axes is increasing. There may also be further effects due to a monopolar particle wind or infalling supernova debris.

Key words: stars: neutron – pulsars: general

1 INTRODUCTION

The slowdown of a rotating neutron star is usually understood to arise from the loss of kinetic rotational energy in the form of electromagnetic radiation from a rotating dipolar magnetic field attached to the star. In this simple model, the slowdown rate of a pulsar in vacuo, rotating at frequency ν , having a magnetic dipole moment M , moment of inertia I and inclination angle α between the magnetic and rotation axes is given by

$$\dot{\nu} = -\frac{8\pi^2 M^2 \sin^2 \alpha}{3c^3 I} \nu^3. \quad (1)$$

If M , I and α are constant, we would expect to observe a dependency of $\dot{\nu} \propto \nu^3$ as the pulsar slows down. However, other braking mechanisms are possible with different dependence upon ν and, in a more general power-law slowdown of the form

$$\dot{\nu} = -\kappa \nu^n, \quad (2)$$

the value of the exponent of ν is known as the braking index n , being 3 for dipolar magnetic torque. Other mechanisms have been proposed which would give lower values of n ; for

example, Michel & Tucker (1969) showed that the torque from a simple outflow of particles would lead to $\dot{\nu} \propto \nu^1$, i.e. $n = 1$. The value of n may also differ from 3 if, for instance, the values of M , α or I in equation (1) vary with time (Blandford & Romani 1988). In order to explore the physics of this slowdown, the value of n can in principle be determined from observation of higher-order frequency derivatives; differentiation of equation (2) shows that the second and third derivatives should be related to n by

$$n = \frac{\ddot{\nu} \nu}{\dot{\nu}^2} \quad \text{and} \quad (3)$$

$$n(2n-1) = \frac{\ddot{\nu} \nu^2}{\dot{\nu}^3}. \quad (4)$$

For most pulsars, evaluation of the rotational slowdown law is confined to measurement of the rotational frequency ν and its first derivative $\dot{\nu}$. For old pulsars, the second derivative $\ddot{\nu}$ expected from equation (3) is usually unmeasurably small, while in many younger pulsars any secular behaviour is often confused by unpredictable changes in rotation rate, in the form of either timing noise or glitches. Timing noise is seen as slow quasi-random changes in rotation rate and arises from magnetospheric instabilities (Lyne et al. 2010), while glitches are almost instantaneous increases in rotation rate, often followed by some associated transient be-

* E-mail: andrew.lyne@manchester.ac.uk

Table 1. Measured braking indices for young pulsars

PSR	n	Reference
B0531+21(Crab)	2.51(1)	Lyne et al. (1993)
B0540–69	2.14(1)	Livingstone et al. (2007)
B0833–45(Vela)	1.4(2)	Lyne et al. (1996)
J1119–6127	2.684(2)	Weltevrede et al. (2011)
B1509–58	2.839(1)	Livingstone et al. (2007)
J1734–3333	0.9(2)	Espinoza et al. (2011b)
J1833–1034	1.857(1)	Roy et al. (2012)
J1846–0258	2.65(1)	Livingstone et al. (2007)

haviour and have their origin in the neutron star interior (Espinoza et al. 2011c).

Because of these effects, values of braking index have been reliably established for only eight pulsars. For the Crab pulsar, $\dot{\nu}$ has been measured between glitches (Lyne et al. 1993), leading to an observed value $n_{\text{obs}} = 2.51(1)$, significantly less than the value of $n = 3$ expected for braking by magnetic dipole radiation. The same is true for all the other seven pulsars (Table 1). These results indicate that the physical process causing the slowdown is not just simple dipolar electromagnetic radiation.

In this paper we report on the measurement and analysis of the rotation rate of the Crab pulsar from 1968 to 2013. This 45-year time-baseline amounts to about 5% of the pulsar lifetime and allows the spin-down of the Crab pulsar to be described over a period which includes many glitches and provides more details of the cumulative effect that they have on the long-term spin-down (Lyne et al. 1993; Smith & Jordan 2003). Elsewhere, the same data have been used to examine the statistics and physical details of the glitches (Espinoza et al. 2014) and to study the evolution of the radio pulse emission over this time (Lyne et al. 2013) to enable a comprehensive picture of the evolution of the pulsar.

2 OBSERVATIONS AND BASIC ANALYSIS

The rotation of the Crab pulsar has been monitored by daily observations at Jodrell Bank Observatory since 1984, mainly using the 13-m radio telescope at 610 MHz (Lyne et al. 1988, 1993). Regular observations with the 76-m Lovell telescope at around 1400-1700 MHz, designed to monitor any changes in dispersion measure, also contribute to the dataset.

These data have been supplemented with earlier observations taken at Arecibo (Gullahorn et al. 1977) and in the optical at Princeton (Groth 1975) and Hamburg (Lohsen 1981). There are no observations available between February 1979 and February 1982, this being the only significant gap with no data. There are in total approximately 11,000 times of arrival (TOAs) and together the measurements comprise a record of the rotation of the pulsar over a total of 45 years from November 1968 to December 2013.

In order to study the long-term rotational history of the pulsar, we have used standard procedures to reduce the TOAs to the barycentre of the Solar System. We have then fitted values of the rotation frequency ν and its first two derivatives $\dot{\nu}$ and $\ddot{\nu}$ over time spans of approximately 100 days. Such analyses were repeated with the central reference

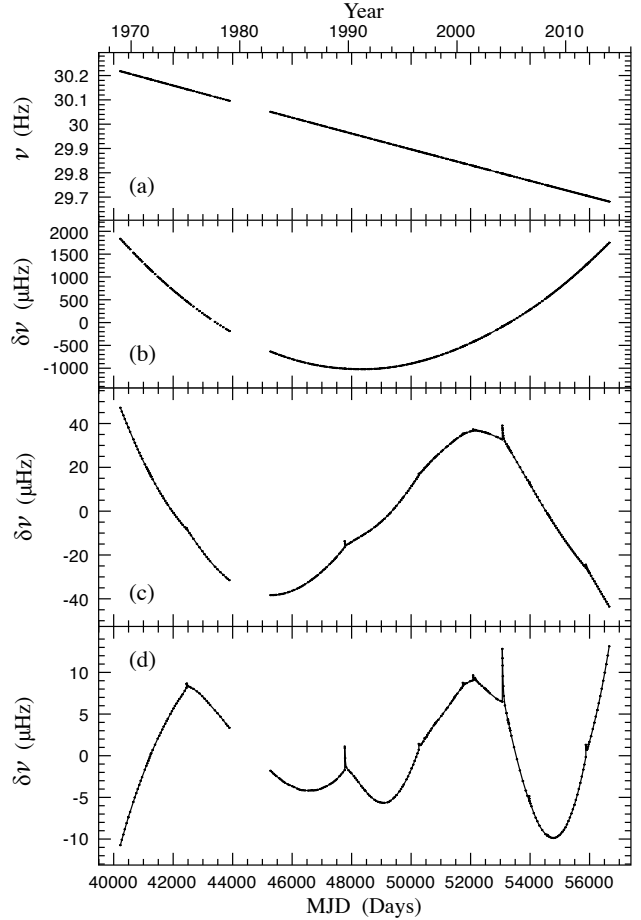


Figure 1. The spin-frequency history of the Crab pulsar over 45 years. (a) The observed spin-frequency ν determined from fits to 100-day data sets every 50 days, showing the monotonic slow-down of the pulsar. (b), (c) and (d) The frequency residuals $\delta\nu$ after fitting to the values in (a) simple slow-down models involving frequency and respectively one, two and three spin-frequency derivatives in the Taylor Series of equation (5). The fitted values of ν_0 , $\dot{\nu}_0$, $\ddot{\nu}_0$ and $\ddot{\nu}_0$ for (d) are given in Table 2.

time advancing by typically 50 days between analyses. Close to glitches, the time spans were adjusted in such a way that no analysis was performed over a glitch, so that one analysis ended and another started close to the epoch of the glitch.

These time sequences of rotational frequencies and first derivatives provide the main forms of the data that we use to study the long-term behaviour of the pulsar in this paper. Figs. 1a and 2a illustrate the evolution of the rotational frequency $\nu(t)$ and slowdown rate $\dot{\nu}(t)$ over the 45 years. The rotational slowdown of the pulsar is evident in Fig. 1a, falling by about 0.5 Hz during this time. The slowdown rate (Fig. 2a) also shows a general reduction in magnitude with time, but there are also considerable long-term effects resulting from glitches, which we investigate further in a later section.

Following convention, it is instructive to characterise the variation in rotation frequency with time as a Taylor series of derivatives of the form:

$$\nu(t) = \nu_0 + \dot{\nu}_0(t-t_0) + \frac{1}{2}\ddot{\nu}_0(t-t_0)^2 + \frac{1}{6}\ddot{\nu}_0(t-t_0)^3 + \delta\nu(t). \quad (5)$$

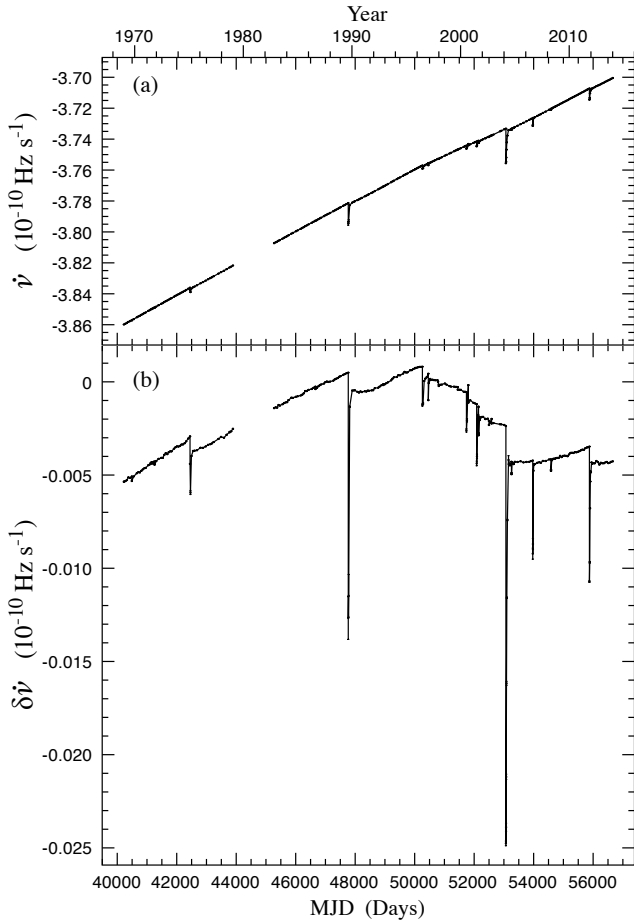


Figure 2. The slowdown rate $\dot{\nu}$ of the Crab pulsar over 45 years. (a) Observed values of the first derivative $\dot{\nu}$ determined from fits to 100-day data sets every 50 days. The magnitude of the slowdown rate $|\dot{\nu}|$ is decreasing overall, with small step increases at the glitches. (b) Frequency derivative residuals $\delta\dot{\nu}$ on an expanded scale, obtained by subtracting from (a) a linear model using the values of the first two frequency derivatives given in Table 2.

By fitting such a model to the frequency data, we evaluate ν_0 and the first three derivatives, leaving a residual $\delta\nu(t)$. In Figs. 1b-1d we see the residuals resulting from fitting and subtracting Taylor series consisting of 1, 2 and 3 derivative terms, respectively. In each case, the residuals are dominated by the next, unfitted derivative term. The remaining residuals shown in Fig. 1d, which might in previous analyses have been designated as timing noise, are related to glitch activity, which we discuss later. The best fit values obtained from the 3-derivative fit are presented in Table 2. These parameters represent the long-term behaviour of the pulsar, including the effects of glitches.

Using equation (3) and the values in Table 2, a braking index $n = 2.349(1)$ is obtained. Using this braking index in equation (4) it is found that the expected value of $\ddot{\nu}$ is $-0.52 \times 10^{-30} \text{ Hz s}^{-3}$, which is about one fifth of the measured value. This shows that the general long-term slowdown of the Crab pulsar is not a simple power-law. We show later that removal of the effects of glitches brings the slowdown close to a simple power-law.

Extrapolating the Taylor series back in time to investigate the behaviour in earlier years should evidently be ap-

Table 2. Observed and derived parameters for the Crab pulsar. The spin parameters were obtained by fitting a 3-derivative Taylor series to the frequency data presented in Fig. 1a. The standard errors determined in the analysis are given in parentheses after the values and are in units of the least significant digit.

Parameter	Value
Data span (MJD)	40175–56665
Epoch t_0 (MJD)	48442.5
ν_0 (Hz)	29.946923(1)
$\dot{\nu}_0$ ($10^{-10} \text{ Hz s}^{-1}$)	-3.77535(2)
$\ddot{\nu}_0$ ($10^{-20} \text{ Hz s}^{-2}$)	1.1147(5)
$\ddot{\nu}_0$ ($10^{-30} \text{ Hz s}^{-3}$)	-2.73(4)
RMS residual (Hz)	0.0000058
Maximum frequency residual (Hz)	0.000013
Mean braking index n	2.342(1)

proached with caution, but we remark that the series indicates an original rotation rate of 58 Hz (a period of 17 milliseconds) at birth in AD 1054.

3 THE 24 GLITCHES

The monotonic rotational slowdown of the Crab pulsar seen in Fig. 1 is occasionally reversed discontinuously at a glitch, in which ν increases by a small step $\Delta\nu$ of order $10^{-9}\nu$ to $10^{-7}\nu$, followed by a nearly complete recovery within about 20 days of the event. The magnitude of the slowdown rate $|\dot{\nu}|$ (Fig. 2) also presents an initial step increase at a glitch, again partially reversing the long-term trend and showing the corresponding short-term recovery (Lyne et al. 1993; Wong et al. 2001). However, in contrast with the relaxation in ν , the recovery in slowdown rate is not complete and a persistent step ($\Delta\dot{\nu}_p$) is commonly observed after glitches. First remarked upon by Gullahorn et al. (1977) and Demiański & Prószyński (1983) in relation to the glitch of 1975, these persistent steps are a general feature of glitches in this pulsar and have an appreciable effect on the overall slowdown behaviour.

Unfortunately, the study of the long-term impact of glitches is often contaminated by the occurrence of other, nearby glitches. However, there are three large glitches which are “isolated”, each having no other detectable glitches within 800 days before or 1200 days after the epoch of the glitch. These three glitches, in 1975, 1989 and 2011 allow the nature of these persistent steps to be demonstrated in Fig. 3. As pointed out by Lyne et al. (1993) in relation to the glitch of 1989, the persistent step increase in slowdown rate consists of an instantaneous component followed by a further quasi-exponential asymptotic increase on a timescale of about 265 days. We now see in Fig. 3 that the same description applies closely to all three large, isolated glitches: all three step changes in $\dot{\nu}$ have different amplitudes and all three show a further increase in $\dot{\nu}$ which grows exponentially for at least a year after the initial step. Additionally, the relative amplitudes of the step and the exponential and the time scales of the exponential are identical to within the fitted errors for all three. As a result, we conclude that the long-term recovery can be represented by a single-parameter function of the form:

$$\delta\dot{\nu} = \begin{cases} 0 & \text{if } t < 0 \\ \Delta\dot{\nu}_p \times (0.46 \times \exp(-t/320) - 1.0) & \text{if } t > 0, \end{cases} \quad (6)$$

where t is the time from the glitch epoch in days and $\Delta\dot{\nu}_p$ is the total persistent step in slowdown rate. Note that the asymptotic exponential is in the same sense as the initial step in $\dot{\nu}$, unlike the short-term recovery at a glitch.

We now regard this as an intrinsic component of all glitches, although for many it is often obscured by the recovery from previous glitches or the occurrence of later glitches. The asymptotic exponential component has a timescale of 320 ± 20 days and comprises 46%, or almost half, of the total increase of slowdown rate. In what follows, we assume that these values apply to all glitches in the Crab pulsar.

Table 3 lists 24 glitches, giving the date and MJD of occurrence, the step change $\Delta\nu$, the fractional value $\Delta\nu/\nu$ and the persistent change of slowdown rate $\Delta\dot{\nu}_p$. This is a robust list which includes all glitches for which $\Delta\nu > 0.01\mu\text{Hz}$. Any glitches smaller than this are of similar size to the period variations produced by the noise present in the data. Any glitch which may have occurred during the gap in observations in 1981 left no obvious change in slowdown rate, and would presumably have been small and would not affect the results of our analysis. Glitch epochs and frequency step sizes were taken from Espinoza et al. (2011c) and Espinoza et al. (2011a). The sequence of glitches is illustrated in Fig. 4a, which shows the date of occurrence and the size $\Delta\nu$ of each glitch (on a logarithmic scale). Note particularly the pattern of substantially increased activity from MJD ~ 50000 to MJD ~ 54000 (years 1995-2006). A histogram of glitch sizes $\Delta\nu$ is shown in Fig. 5a. Espinoza et al. (2014) have analysed the Jodrell Bank data on the Crab pulsar and conclude that the decrease in numbers of glitches towards smaller sizes is intrinsic and is not related to the detection capabilities.

The persistent steps in frequency derivative were estimated by fitting a function of the form given by equation (6) to the observed $\dot{\nu}$ data centred on the glitch epoch. In order to avoid contamination by short-term glitch transient recoveries, data taken within 90 days following each glitch were not used. In some cases the step is very small and no significant measurement was possible. In other cases, because of the presence of other nearby glitches, the available data points were insufficient to perform the measurement, although in a few cases it was possible to measure the combined effect of two or three closely-separated glitches (Table 3). Without being extremely precise, this method effectively measures the basic trends we are studying and it is not affected by the necessary assumptions of more complicated models. Our values are roughly consistent with existent measurements using such models (e.g. Wong et al. 2001; Wang et al. 2012).

The step in $\Delta\dot{\nu}_p$ at a glitch is loosely related to the step-change in rotation frequency $\Delta\nu$. The relationship is shown in Fig. 5b, which includes data from 15 glitches (some points combine data from two or three adjacent glitches). The approximately linear relationship is fitted by the diagonal line of unity slope, given by

$$|\Delta\dot{\nu}_p| = 7 \times 10^{-8} \times \Delta\nu \text{ Hz s}^{-1}, \quad (7)$$

where $\Delta\nu$ is in Hz.

The persistent slowdown increase is usually attributed

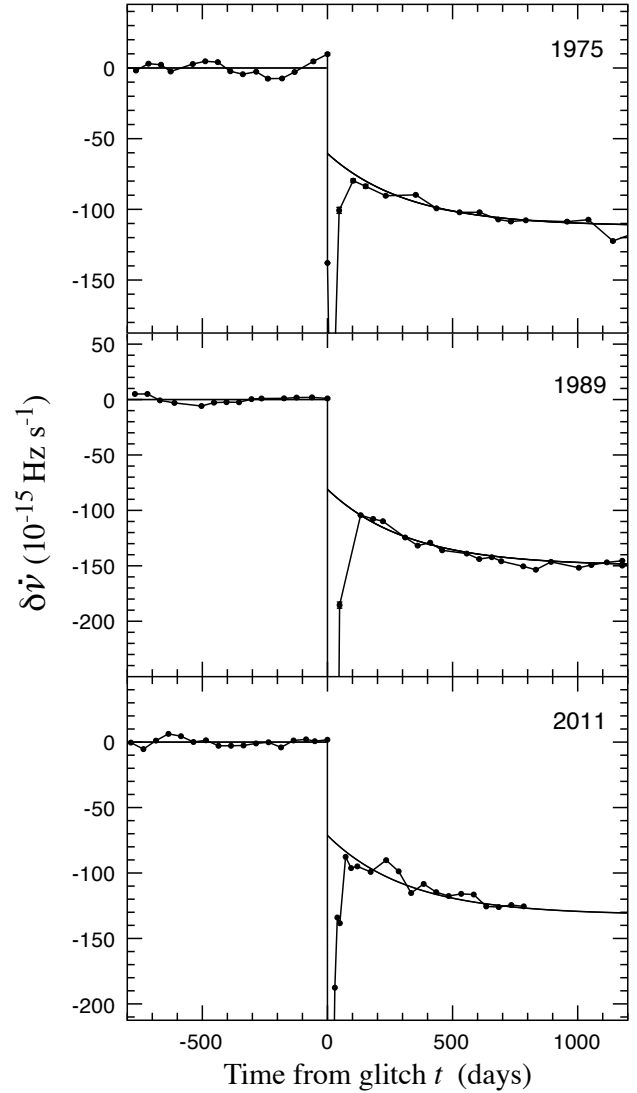


Figure 3. The variation in slowdown rate $\dot{\nu}$ of the Crab pulsar near to the three large isolated glitches which occurred in 1975, 1989 and 2011. In each case, the frequency derivative residuals $\delta\dot{\nu}$ were obtained relative to a linear model involving the first two frequency derivatives fitted to $\dot{\nu}$ over the 800 days preceding the glitch, which occurred at day 0. Each glitch is followed instantly by a large negative transient (increase in magnitude) in $\dot{\nu}$. The main transient behaviour ceases after about 100 days, revealing a persistent negative offset which continues to increase in a quasi-exponential manner on a timescale of around 320 days. The smooth lines are the fits to the post-glitch data described by equation 6.

to a reduction in effective moment of inertia due to pinning of neutron superfluid vortices to other internal components. Because a rotating superfluid slows down only if its vortices are allowed to move apart, the pinning of some vortices decouples a fraction of the superfluid from the rest of the star and reduces the effective moment of inertia of the rotating star. Equation (7) indicates that the re-pinning of vortices is more effective after larger glitches.

We offer no explanation for the surprising phenomenon of the long-term asymptotic increase in $\dot{\nu}$ and continue to view all increases of slowdown rate at glitches as decreases in

Table 3. The steps in rotation rate and slowdown rate for the 24 glitches observed between 1968 and 2013. This table is derived from Espinoza et al. (2014)

Date	MJD days	$\frac{\Delta\nu}{\nu}$ 10^{-9}	$\Delta\nu$ μHz	$\Delta\dot{\nu}_p$ 10^{-15}s^{-2}
1969 Sep	40491.84(3)	7.2(4)	0.22(1)	—
1971 Jul	41161.98(4)	1.9(1)	0.057(4)	—
1971 Oct	41250.32(1)	2.1(1)	0.062(3)	—
1975 Feb	42447.26(4)	35.7(3)	1.08(1)	−112(2)
1986 Aug	46663.69(3)	6(1)	0.18(2)	—
1989 Aug	47767.504(3)	81.0(4)	2.43(1)	−150(5)
1992 Nov	48945.6(1)	4.2(2)	0.13(1)	—
1995 Oct	50020.04(2)	2.1(1)	0.063(2)	—
1996 Jun	50260.031(4)	31.9(1)	0.953(4)	*
1997 Jan	50458.94(3)	6.1(4)	0.18(1)	−116(5) [†]
1997 Dec	50812.59(1)	6.2(2)	0.19(1)	—
1999 Oct	51452.02(1)	6.8(2)	0.20(1)	−25(3)
2000 Jul	51740.656(2)	25.1(3)	0.75(1)	*
2000 Sep	51804.75(2)	3.5(1)	0.105(3)	−53(3) [†]
2001 Jun	52084.072(1)	22.6(1)	0.675(3)	*
2001 Oct	52146.7580(3)	8.87(5)	0.265(1)	−70(10) [†]
2002 Aug	52498.257(2)	3.4(1)	0.101(2)	*
2002 Sep	52587.20(1)	1.7(1)	0.050(3)	−8(2) [†]
2004 Mar	53067.0780(2)	214(1)	6.37(2)	*
2004 Sep	53254.109(2)	4.9(1)	0.145(3)	*
2004 Nov	53331.17(1)	2.8(2)	0.08(1)	−250(20) ^{††}
2006 Aug	53970.1900(3)	21.8(2)	0.65(1)	−30(5)
2008 Apr	54580.38(1)	4.7(1)	0.140(4)	—
2011 Nov	55875.5(1)	49.2(3)	1.46(1)	−132(5)

[†]incorporates the persistent step of the previous glitch.

^{††}incorporates the persistent steps of the previous two glitches.

effective moment of inertia, presumably due to vortex pinning. We note that if there is no relaxation in this cumulative pinning, the proportional change in moment of inertia has amounted to 0.3% in 45 years. We remark that such a large rate of change cannot persist for more than a few thousand years, by which time a large proportion of the effective moment of inertia of the neutron star would have disappeared.

Melatos et al. (2008) include the Crab pulsar glitches in a comprehensive analysis of the statistics of the distributions of size and intervals between glitches, testing the hypothesis that these are determined by a random process of self-organised criticality. The incidence of glitches in most pulsars appears to be random, and Wang et al. (2012) show that the distribution of interval times in the Crab pulsar is Poissonian, although some pulsars show a quasi-periodicity (Link et al. 1999; Melatos et al. 2008; Wang et al. 2012).

We nevertheless draw attention to the cluster of 15 glitches between MJD 50000 and 54000 seen in Fig. 4, which suggests that there may be an extra complexity in the system. We require a statistical test for the hypothesis that this cluster was a chance concentration of glitches which occurred at random. The Wang et al. (2012) test was not sensitive to clustering, which is better revealed by the distribution of intervals between all glitches, rather than only consecutive ones. We therefore compare the observed distribution of intervals between all glitches with those from simulated glitch

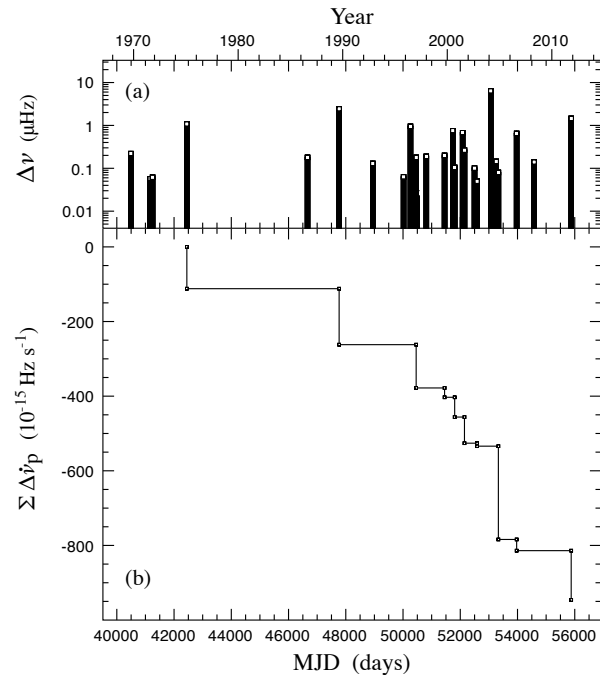


Figure 4. Glitches in the Crab pulsar. (a) The distribution in time and magnitude of the steps $\Delta\nu$ in spin-frequency of the 24 glitches in Table 3. (b) The cumulative effect of the persistent steps in slowdown rate $\Delta\dot{\nu}_p$ at the glitches.

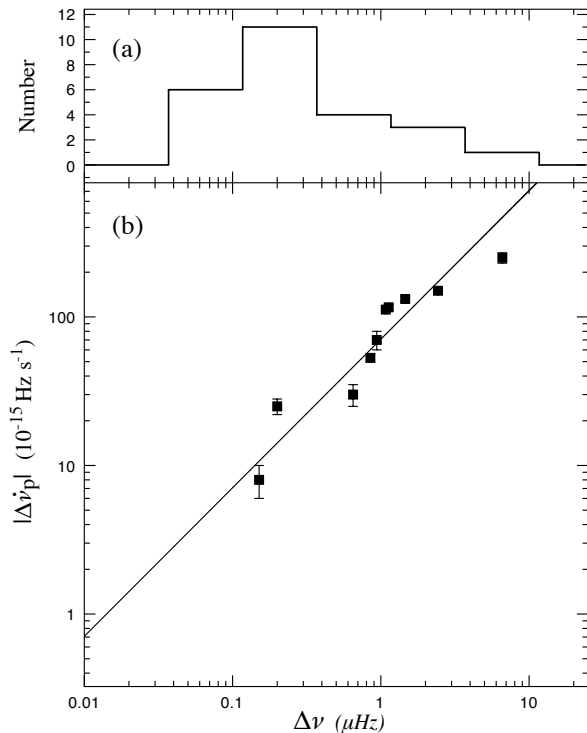


Figure 5. Glitch sizes. (a) Histogram of frequency steps $\Delta\nu$ on a logarithmic scale for the 24 glitches in Table 3. (b) The interdependence of the persistent change in slow-down rate $|\Delta\dot{\nu}_p|$ and the step-change in rotation frequency $\Delta\nu$ for 10 glitches. The diagonal line has a slope of unity. Only events for which $\Delta\dot{\nu}_p < 0$ are shown.

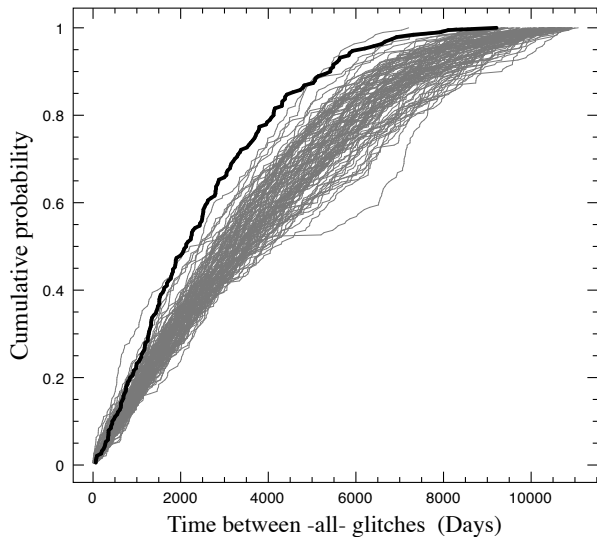


Figure 6. The cumulative distribution of intervals between all 20 glitches occurring between MJD 46000 and MJD 56600, as observed (bold line) and in 100 random simulations.

sequences and show that the probability that the observed distribution is random is low.

We confined our analysis to the 20 glitches which occurred in the last 30 years since high-cadence monitoring commenced in January 1984. As explained in Espinoza et al. (2014), the data in this period constitute a uniform set and are complete, indicating a mean rate of 0.67 glitches/yr. The bold line in Figure 6 shows the cumulative distribution of all 190 glitch separation times in this set of data. We then generated 10,000 simulated distributions of 20 events, each occurring at a random time within a 30-year period; in Fig. 6, we show 100 of these realisations (randomly picked) for comparison with the observed distribution.

The curve derived from the observed data lies on the outside of the spread of curves from the simulations, indicating a low probability that the observed cluster was a random occurrence. In particular, there is an excess of small separation times in the observed cumulative distribution, which is therefore steeper than most of the simulated distributions. This indicates that the glitches are more clustered than can be expected from a random occurrence of glitches. We also compared the means of the separation times in the distributions; the mean of the 190 observed glitch separation times was less than the mean in all except 52 (0.5%) of the 10,000 simulated distributions. We therefore conclude that it is unlikely that the cluster of glitches is a statistical accident. We note that the 11-year period of the cluster coincides with a period of an anomaly in the underlying slowdown rate, which is seen in Fig. 7 and will be discussed in the next Section.

4 THE EFFECT OF GLITCHES ON THE SLOWDOWN

Fig. 4b shows the cumulative effect of the steps $\Delta\dot{\nu}_p$ at the 17 glitches for which this quantity was measured. The total cumulative effect over 45 years is an increase in slow-

down rate $|\Sigma\Delta\dot{\nu}_p|$ of $946(25) \times 10^{-15} \text{ Hz s}^{-1}$. The small but appreciable overall negative contribution made by the glitches to the second derivative $\ddot{\nu}$ may be evaluated by dividing the total sum by the time interval, giving a value of $-0.066(4) \times 10^{-20} \text{ Hz s}^{-2}$, which is approximately 6% of the second derivative $\ddot{\nu}$ evaluated from the long-term analysis (Table 2).

We now address the notion that the slowdown is an underlying steady phenomenon with superimposed cumulative steps in the slowdown rate caused by glitches. If the persistent steps $\Delta\dot{\nu}_p$, as tabulated in Table 3 and with the form described by equation 6, are removed from the $\dot{\nu}$ data we obtain a smoother, “corrected” $\dot{\nu}$ evolution which shows the underlying slowdown. Fig. 7a shows frequency derivative residuals obtained by removing from the corrected $\dot{\nu}$ data a new linear 2-term Taylor series fitted to the restricted 6-year span up to MJD 42447, this being the epoch of the 1975 glitch. This fit yields values of $\dot{\nu} = -3.84796(1) \times 10^{-10} \text{ Hz s}^{-1}$ and $\ddot{\nu} = 1.236(1) \times 10^{-20} \text{ Hz s}^{-2}$ at MJD 41338.67. We now find from equation (3) that during this span, the braking index was $n = 2.519(2)$, and from equation (4) the expected value of $\ddot{\nu} = -0.636(1) \times 10^{-30} \text{ Hz s}^{-3}$. The smooth curve in Fig. 7a is the calculated variation in $\dot{\nu}$ including the curvature due to this term, and in general is seen to track the data well.

However, at around MJD 50000, the slope in Fig. 7a changes abruptly, recovering at around MJD 54000, after an accumulated offset in $\dot{\nu}$, to approximately the expected slope. This is the same 11-year span that contains the large concentration of glitches. The accumulated deviation in this 11-year span amounts to $\sim -200 \times 10^{-15} \text{ Hz s}^{-1}$, and is in addition to the $\sim -522 \times 10^{-15} \text{ Hz s}^{-1}$ already accounted for by the observed persistent glitch contributions $\Delta\dot{\nu}_p$ in this period, and may be compared with the total change during this time of $\sim 3500 \times 10^{-15} \text{ Hz s}^{-1}$ due to the underlying slowdown. It seems unlikely that the deviation can be due to glitches which are below the threshold of our measurements, since Fig. 5a shows a deficit of small glitches (Espinoza et al. 2014). More likely, the accumulated deviation is due to a phenomenon related to glitches which is not reflected in our present model.

The variations in $\delta\dot{\nu}$ may also be interpreted as changes in the underlying value of the braking index n with time. These changes are summarised in Fig. 7b, in which the value of the braking index is close to 2.5 throughout most of the 45 years, except for the period of high glitch activity from MJD 50000-54000, when it takes a value of about 2.3.

We remark that the process of separating the effects of glitches from an underlying steady rotational evolution provides a good description of the overall behaviour, with braking index $n = 2.5$. The small effect on the index seen in Fig. 7b remains unexplained.

5 THE SLOWDOWN POWER LAW

Why is the braking index different from 3, as expected from equation (1) for energy loss through electromagnetic dipole radiation? Either this equation is inadequate because angular momentum is also lost through a mechanical process such as an outflowing jet or interaction with an external fall-back disk of supernova remains (Menou et al. 2001), or

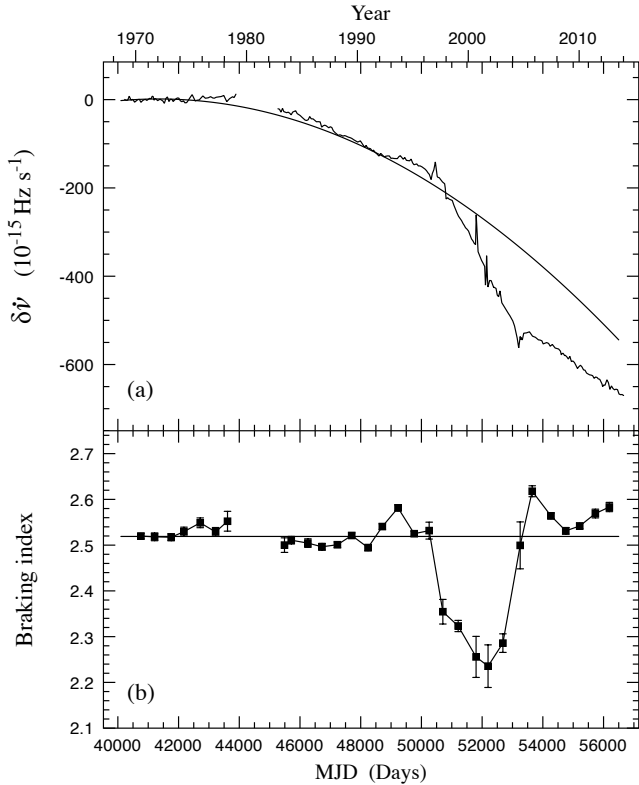


Figure 7. The underlying slowdown of the Crab pulsar after removal of the effects of the glitches. a) The frequency derivative residuals $\delta\dot{\nu}$ obtained by subtracting from $\dot{\nu}$ data the persistent steps $\Delta\dot{\nu}_p$ at the glitches given in Table 3, removing short-term glitch transients by excluding data within 90 days following each glitch, and by removing the main linear trend as measured from the start to MJD 50458. The smooth curve is the expected behaviour during this era for a constant value of $n = 2.519$, showing a curvature corresponding to a value of $\ddot{\nu} = -0.636 \times 10^{-30} \text{ Hz s}^{-3}$ as calculated from equation (4). b) The underlying braking index of the Crab pulsar using equation 3, evaluated over sections of 1000 days at 500-day intervals. The values of ν and $\dot{\nu}$ are the mean values of the data in each interval in Figs. 1a and 2a, and $\ddot{\nu}$ is taken from the slope of the corresponding data in (a). The horizontal line at $n = 2.519$ corresponds to the curve in (a).

one or more of the parameters I , M , or α of the equation is changing with time. These two categories might be called the unipolar and dipolar approaches in which the loss of angular momentum may lead to very different slowdown laws $\dot{\nu} \propto \nu$ and $\dot{\nu} \propto \nu^3$ respectively. As pointed out by Harding et al. (1999), Xu & Qiao (2001), and Chen & Li (2006), a combination of both processes could account for the observed low braking indices of young pulsars.

5.1 The wind component

The Crab pulsar, along with other young pulsars, generates a powerful particle stream whose effect is observed as a wind nebula (e.g. Gaensler & Slane (2006)). The possible effect of angular momentum carried away by this particle stream has been much debated, following Michel & Tucker (1969) who pointed out that if the slowdown were predominantly due to wind, the torque would follow the first rather than the third power of the rotation rate. Other values of braking

index of less than three due to particle flows have also been suggested (e.g. Wu et al. (2003)). An alternative approach by Menou et al. (2001) suggests that interaction between the rotating pulsar and an accretion disc of infalling supernova remains, forming outside the magnetosphere but coupled by a propeller torque, would lead to a similar slowdown law. Yan et al. (2012) consider the effect of this process on the timing properties of old as well as young pulsars.

For instance, if the departure of the braking index from 3 is due to such a dynamic process with braking index $n = 1$, the slowdown can be represented by a combination of two power laws:

$$\dot{\nu} = -(A\nu^3 + B\nu). \quad (8)$$

If at the present time the dynamic component increases the slowdown rate by a factor $(1 + \epsilon) = (1 + B/A\nu^2)$, it is easy to show that the observed braking index is

$$n = \frac{\nu\ddot{\nu}}{\dot{\nu}^2} = \frac{\epsilon + 3}{\epsilon + 1} \quad (9)$$

and

$$\epsilon = \frac{3 - n}{n - 1}. \quad (10)$$

If the wind (or the disk) was to be responsible for the whole of the difference between $n_{\text{dip}} = 3$, the expected value from magnetic-dipole braking, and n_{obs} , the observed value, then equation (10) shows that for $n_{\text{obs}} = 2.5$, the wind accounts for approximately one third of the slowdown torque. A more precise modelling of the effect of the wind or disk might lead to a more accurate assessment of this proportion. For the Vela pulsar, the very low value of $n_{\text{obs}} = 1.4$ suggests that the wind is responsible for $\frac{4}{5}$ of the slowdown torque.

5.2 A changing magnetic dipole

If alternatively the low braking index is predominantly due to magnetic dipole radiation in which the coefficient κ in equation (2) is a function of time $\kappa(t)$, then the observed braking index will be

$$n_{\text{obs}} = \frac{\ddot{\nu}\nu}{\dot{\nu}^2} = n_{\text{dip}} + \frac{\dot{\kappa}(t)\nu}{\kappa(t)\dot{\nu}}. \quad (11)$$

The observed interglitch value of braking index for the Crab pulsar, $n_{\text{obs}} = 2.5$, would require $\dot{\kappa}/\kappa \simeq 2.0 \times 10^{-4} \text{ yr}^{-1}$. Since

$$\kappa \propto M^2 \sin^2 \alpha I^{-1}, \quad (12)$$

we evaluate the changes in these three parameters which might account for the low value of the braking index.

From equation (11) the effects are given by

$$n_{\text{obs}} = n_{\text{dip}} + \frac{\nu}{\dot{\nu}} \left(-\frac{\dot{I}}{I} + 2\frac{\dot{\alpha}}{\tan \alpha} + 2\frac{\dot{M}}{M} \right). \quad (13)$$

The overall changes in the Crab slowdown are too large to be explained by simple changes in ellipticity and the consequent changes in the moment of inertia I of a rotating ellipsoid. An apparent reduction in I might however be due to a continuous decoupling of the interior produced by an accumulation of pinned vortices in reservoirs (Alpar et al. 1996; Ho & Andersson 2012), eventually locking up a substantial fraction of the superfluid. Such a process would eventually

be limited by the available superfluid, which is usually considered to be the superfluid in the neutron-rich inner crust. It seems unlikely that the process could persist long enough to explain the low braking index of older pulsars such as the Vela pulsar.

Several authors, notably Blandford & Romani (1988); Chen et al. (1998); Allen & Horvath (1997); Lyne (2004); Espinoza et al. (2011b), have remarked that a low braking index might be due to an increasing dipolar magnetic field, or to an increasing inclination angle α . Evidence for a secular increase in α has been presented by Lyne et al. (2013). From observations of the profile of the radio pulse over 22 years, they find an increase in the component separation amounting to 6×10^{-3} degrees per year. They remark that this can be attributed to a similar rate of increase in α , which for $\alpha = 45$ deg would account for the low value of the braking index. Using the long-term value of $n_{obs} = 2.35$, they found that the changing α gives a value of $\dot{\kappa}/\kappa = 2.6 \times 10^{-4} \text{ yr}^{-1}$, which could account for the observed rate of change.

However, although the secular change in α may well be sufficient to account for the whole of the reduction in the value of the braking index below 3, it should be noted that the determination of $\dot{\alpha}$ from the observation of the separation of the components of the pulse profile is model dependent. Hence the actual contribution is uncertain and it is also likely that the relative contributions of the different processes discussed above may be evolving with time. Further possibilities are models of pulsar magnetospheres which recognise an inner region corotating with the star and which can lead to $n < 3$ when the evolution of this region's size changes at a different rate to the constantly-growing light cylinder region (Melatos 1997; Contopoulos & Spitkovsky 2006; Bucciantini et al. 2006).

6 LONG-TERM EVOLUTION AND THE $P - \dot{P}$ DIAGRAM

The departure from simple magnetic dipole slowdown is illustrated dramatically in Fig. 8. This shows a section of the familiar $P - \dot{P}$ diagram, a log-log plot on which it is customary to plot all known pulsars. As a pulsar ages, it moves from left to right across the diagram, following a path whose slope $2 - n$ depends on the braking index. For $n = 3$, the slope is -1 . For the Crab pulsar, for which the mean value of $n = 2.349$, the slope is ~ -0.35 , representing the general movement of the Crab pulsar on the diagram. However, between glitches the evolution is with a slope of -0.5 , corresponding to $n = 2.5$. If the wind model is correct, the monopole term will eventually dominate and the path across the $P - \dot{P}$ diagram will turn upwards towards a slope of $+1$. As pointed out by Alvarez & Carramiñana (2004), this leads into a region of the diagram where no pulsars have been detected; however, it does lead towards the magnetars (Espinoza et al. 2011b). Harding et al. (1999) remark on the possibility that the high slowdown rate of the magnetars may be accounted for largely or completely by monopolar wind torque, in contrast to the current interpretation in terms of a very high dipole magnetic field.

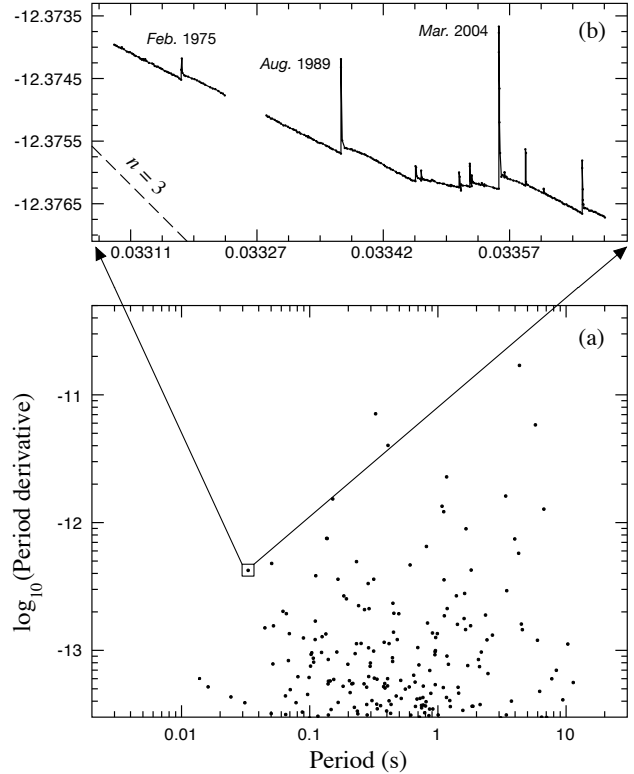


Figure 8. The progress of the Crab Pulsar across the $P - \dot{P}$ diagram. a) The upper part of the standard $P - \dot{P}$ diagram and b) an expanded view of the region containing the Crab Pulsar, showing its motion during the past 45 years. The dot-dash line represents the path that would be followed by a pulsar having braking index $n = 3$.

7 CONCLUSIONS

The slowdown of the rotation rate of the Crab pulsar, including the effect of the glitches, could be described by a power law with braking index of around 2.35. The spin evolution is, however, affected by the steps in slowdown rate at glitches; removing these reveals an underlying simple slowdown with braking index 2.519(2). The average effect of the glitches is to increase the rate of slowdown by about 6%. This description of the slowdown fails during a 11-year period which coincides with a period of increased glitch activity.

Including the exponential component of the persistent step in slowdown rate at glitches allows an almost complete separation of the effects of glitches from the underlying slowdown. This component is in the form of an exponential with time constant 320 days, asymptotically reaching a value which nearly doubles the previously known effect.

The $n = 2.5$ braking index, lower than the conventional value $n = 3$ for a rotating magnetic dipole, may be attributed to a combination of a secular increase in magnetic inclination angle and a monopolar wind torque. If the rate of mass loss in the wind persists, the braking index is expected to reduce towards $n = 1$, possibly accounting for the low index observed in the Vela pulsar.

The observed pattern of glitch activity, including the 11-year period of increased glitch activity, does not agree well

with the random behaviour expected from self-organised criticality.

ACKNOWLEDGEMENTS

Pulsar research at JBCA is supported by a Consolidated Grant from the UK Science and Technology Facilities Council (STFC). C.M.E. acknowledges the support from STFC and FONDECYT (postdoctorado 3130512).

REFERENCES

- Allen M. P., Horvath J. E., 1997, *ApJ*, 488, 409
 Alpar M. A., Chau H. F., Cheng K. S., Pines D., 1996, *ApJ*, 459, 706
 Alvarez C., Carramiñana A., 2004, *A&A*, 414, 651
 Blandford R. D., Romani R. W., 1988, *MNRAS*, 234, 57P
 Bucciantini N., Thompson T. A., Arons J., Quataert E., Del Zanna L., 2006, *MNRAS*, 368, 1717
 Chen K., Ruderman M., Zhu T., 1998, *ApJ*, 493, 397
 Chen W. C., Li X. D., 2006, *aa*, 450, L1
 Contopoulos I., Spitkovsky A., 2006, *ApJ*, 643, 1139
 Demiański M., Prószczyński M., 1983, *MNRAS*, 202, 437
 Espinoza C. M., Antonopoulou D., Stappers B. W., Watts A., Lyne A. G., 2014, *MNRAS*, 440, 2755
 Espinoza C. M., Jordan C., Bassa C., Janssen G., Lyne A. G., Smith F. G., Stappers B. W., Weltevrede P., 2011a, *The Astronomer's Telegram*, 3777, 1
 Espinoza C. M., Lyne A. G., Kramer M., Manchester R. N., Kaspi V., 2011b, *ApJ*, 741, 13
 Espinoza C. M., Lyne A. G., Stappers B. W., Kramer M., 2011c, *MNRAS*, 414, 1679
 Gaensler B. M., Slane P. O., 2006, *Ann. Rev. Astr. Ap.*, 44, 17
 Groth E. J., 1975, *ApJS*, 29, 431
 Gullahorn G. E., Isaacman R., Rankin J. M., Payne R., 1977, *AJ*, 82, 309
 Harding A. K., Contopoulos I., Kazanas D., 1999, *ApJ*, 525, L125
 Ho W. C. G., Andersson N., 2012, *Nature Physics*, 8, 787
 Link B., Epstein R. I., Lattimer J. M., 1999, *Phys. Rev. Lett.*, 83, 3362
 Livingstone M. A., Kaspi V. M., Gavriil F. P., Manchester R. N., Gotthelf E. V. G., Kuiper L., 2007, *Astrophys. Space Sci.*, 308, 317
 Lohsen E. H. G., 1981, *A&AS*, 44, 1
 Lyne A., Hobbs G., Kramer M., Stairs I., Stappers B., 2010, *Science*, 329, 408
 Lyne A. G., 2004, in *Young Neutron Stars and Their Environments*, IAU Symposium 218, Camilo F., Gaensler B. M., eds., Astronomical Society of the Pacific, San Francisco, pp. 257–260
 Lyne A. G., Graham-Smith F., Weltevrede P., Jordan C. A., Stappers B. W., 2013, *Science*, 342, 598
 Lyne A. G., Pritchard R. S., Graham-Smith F., Camilo F., 1996, *Nature*, 381, 497
 Lyne A. G., Pritchard R. S., Smith F. G., 1988, *MNRAS*, 233, 667
 Lyne A. G., Pritchard R. S., Smith F. G., 1993, *MNRAS*, 265, 1003
 Melatos A., 1997, *MNRAS*, 288, 1049
 Melatos A., Peralta C., Wyithe J. S. B., 2008, *ApJ*, 672, 1103
 Menou K., Perna R., Hernquist L., 2001, *ApJ*, 554, L63
 Michel F. C., Tucker W. H., 1969, *Nature*, 223, 277
 Roy J., Gupta Y., Lewandowski W., 2012, *MNRAS*, 424, 2213
 Smith F. G., Jordan C., 2003, in *ASP Conf. Ser. 302: Radio Pulsars*, Bailes M., Nice D. J., Thorsett S. E., eds., p. 231
 Wang J., Wang N., Tong H., Yuan J., 2012, *Astrophys. Space Sci.*, 340, 307
 Weltevrede P., Johnston S., Espinoza C. M., 2011, *MNRAS*, 411, 1917
 Wong T., Backer D. C., Lyne A., 2001, *ApJ*, 548, 447
 Wu F., Xu R. X., Gil J., 2003, *A&A*, 409, 641
 Xu R. X., Qiao G. J., 2001, *ApJ*, 561, L85
 Yan T., Perna R., Soria R., 2012, *MNRAS*, 423, 2451